

# Full and partial controllability of the Kermack-Mckendrick system with time-varying incidence rates

Hamza El Mahjour<sup>†\*</sup>, Aadil Lahrouz<sup>‡</sup>, Omar Zakary<sup>§</sup> and Mariam Redouane<sup>‡</sup>.

<sup>†</sup> ENSAT, Abdelmalek Essaadi University, Tetouan, Morocco.

<sup>‡</sup> FSTT, Abdelmalek Essaadi University, Tetouan, Morocco.

<sup>§</sup> FSBM, University Hassan II, Casablanca, Morocco

Email(s): h.elmahjour@uae.ac.ma

**Abstract.** This study contributes to the expanding body of literature on epidemic control by introducing a time-varying incidence rate and establishing the global controllability of the resulting nonlinear SIR system. The findings offer a practical framework for public health policymakers to design adaptive and optimized control strategies to mitigate the impact of infectious diseases. Additionally, we explore the partial controllability problem by deriving explicit solutions for the system with control. These solutions demonstrate the feasibility of controlling the infected population at any given time, providing both a robust theoretical foundation and practical guidance for managing infectious disease outbreaks. To further advance practical implementation, we develop numerical methods that exploit an algorithmic approach to achieve full control of the system, targeting a desired state  $(S_d, I_d)$ . Moreover, we propose a novel hybrid method that integrates the analytical solutions derived for partial control with an algorithmic strategy. This hybrid approach leverages the explicit expressions for  $I(t)$  and  $S(t)$  to guide the numerical optimization of control parameters, enhancing the precision and efficiency of epidemic control strategies. By bridging theoretical controllability, analytical insights, and numerical techniques, this work advances the broader goal of developing adaptive and effective approaches to epidemic management.

**Keywords:** Epidemic model, varying infection rate, full control, partial control, hybrid method.

**AMS Subject Classification 2010:** 93C15; 34H05; 92D30.

## 1 Introduction

Infectious diseases remain a leading cause of mortality worldwide, impacting millions of individuals annually [21]. Despite significant advancements in medical research, including the development of vaccines and therapeutic interventions, infectious diseases continue to present substantial public health challenges. The emergence of novel pathogens and the re-emergence of drug-resistant strains further highlight the necessity for global initiatives in disease prevention, epidemiological surveillance and rapid response

\*Corresponding author

Received: 12 August 2025/ Revised: 04 December 2025/ Accepted: 15 December 2025

DOI: [10.22124/jmm.2025.31390.2818](https://doi.org/10.22124/jmm.2025.31390.2818)

strategies. To better understand and predict the spread of infectious diseases, numerous mathematical models have been developed to describe the dynamics of epidemics within populations. Among these, compartmental models based on differential equations, either deterministic or stochastic, are widely utilized. These models typically partition the population into distinct compartments, with the most fundamental classification being the susceptible, infected, and recovered groups. The temporal evolution of these compartments is described by functions  $S(t)$ ,  $I(t)$  and  $R(t)$  that represent the density of individuals in each category at a given time  $t$ . One of the earliest and most influential models was introduced by Kermack and Mckendrick [20], formulated as follows:

$$\begin{cases} \frac{dS}{dt} = -\beta S(t)I(t), \\ \frac{dI}{dt} = \beta S(t)I(t) - \lambda I(t), \\ \frac{dR}{dt} = \lambda I(t). \end{cases} \quad (1)$$

This system of differential equations describes the dynamics of the population densities across the three compartments, incorporating the transmission rate  $\beta$  and recovery rate  $\lambda$ . The propagation of the epidemic is primarily driven by interactions between infected and susceptible individuals, with transmission assumed to occur uniformly throughout the population. Based on the law of mass action, the rate at which new infections arise at any given time is directly proportional to the product of the densities of susceptible and infected individuals, expressed as  $\beta S(t)I(t)$  [6]. Consequently, at any given time  $t$ ,  $\beta S(t)I(t)$  individuals transition from the susceptible compartment to the infected compartment. Simultaneously, infected individuals recover at a rate  $\lambda I(t)$  moving into the recovered compartment, where they acquire permanent immunity. The model formalized in (1) has been the focus of extensive scholarly analysis and has been re-examined from diverse theoretical and applied perspectives. It stands as a cornerstone in the field of epidemiology, providing a foundational structure for the development of numerous subsequent models, as documented in the works of [2, 5, 7], among others. A pivotal concept in epidemic theory is the basic reproduction number  $\mathcal{R}_0$  [10]. It is a dimensionless parameter central to understanding disease transmission dynamics [11, 17]. In the Kermack-McKendrick model,  $\mathcal{R}_0$  is defined as

$$\mathcal{R}_0 = \frac{\beta S_0}{\lambda},$$

where  $S_0$  is the initial susceptible population. The value of  $\mathcal{R}_0$  determines epidemic potential: if  $\mathcal{R}_0 > 1$ , the disease spreads, indicating an epidemic; if  $\mathcal{R}_0 \leq 1$ , it declines, preventing widespread transmission. Another key metric is the final size of an epidemic, representing the fraction of the population remaining susceptible after the outbreak. The final size equation in Kermack-McKendrick framework is derived as [1, 5]:

$$1 - S_\infty - \frac{\lambda}{\beta} \ln \left( \frac{S_0}{S_\infty} \right) = 0, \quad (2)$$

where  $S_\infty$  denotes susceptibles at the epidemic's end. This equation expresses the proportion of the population that avoids infection,  $\frac{S_\infty}{S_0}$ , and the proportion that becomes infected  $\left(1 - \frac{S_\infty}{S_0}\right)$ , offering critical insights for evaluating disease impact and guiding public health strategies [5].

A crucial question that emerges during any epidemic outbreak is whether it can be effectively control-

lable? Controllability, in this context, refers to the capacity to steer a dynamic system from an arbitrary initial state to a desired final state through the application of appropriate control inputs [19, 24]. The controllability of epidemic models has been the subject of many investigations [9, 22, 26, 27]. For instance, Zakary et al. [27] introduced a partial control function designed to improve infection management within a nonlinear SIR epidemiological model. Their approach included deriving explicit solutions and calibrating control parameters to meet specific predefined objectives, particularly regulating the number of infected individuals and ensuring their convergence to a set threshold at a predetermined time, regardless of initial conditions. In a similar vein, Dehaj et al. [9] applied a comparable methodology within a nonlinear SIR model, incorporating two control variables: the vaccination rate for susceptible individuals and the treatment rate for infected individuals per unit time. Moreover, if the study emphasizes cost-effectiveness in epidemic control, optimal control strategies—widely studied in the literature and refined through numerous contributions—should be employed for managing infectious diseases. In this regard, a recent study by Balderrama et al. [3] explores optimal control strategies within an SIR model under the constraint of a limited quarantine duration. The study seeks to minimize both the cumulative number of infections and the socioeconomic costs incurred due to non-pharmaceutical interventions, such as social distancing and quarantine measures. The authors introduce a time-dependent reproduction number,  $\sigma(t)$ , which can be adjusted to account for varying levels of quarantine strictness over a fixed intervention period  $T$ . The most stringent quarantine, characterized by a lower bound  $\sigma_s$ , is constrained to a maximum duration  $\tau < T$ . In [4], Boujallal et al. introduced a novel control set-valued approach for epidemic modeling, employing viability theory and Lyapunov functions to minimize the prevalence of infection. This methodology involves the formulation of feedback maps and continuous selections to derive optimal control strategies, with theoretical guarantees ensuring their existence and efficacy. The proposed approach has been implemented in a controlled SIRS epidemic model, demonstrating a substantial reduction in the number of infected individuals through the application of prevention and treatment measures.

In the present paper, we aim to revisit the classical SIR epidemic model by introducing a time-varying control parameter, represented by the incidence rate  $\beta(t)$ . This approach allows us to consider the dynamic nature of disease transmission and offers greater flexibility in capturing the temporal variations observed in real-world epidemics. Rather than assuming a constant incidence rate, as is typically the case in traditional SIR models, we treat  $\beta(t)$  as a bounded function that can evolve over time, reflecting various external factors influencing the rate of infection. These factors include, but are not limited to, policy interventions such as social distancing measures, vaccination campaigns, the level of public awareness, seasonal variations, and the mobility of individuals [8]. Hence, this approach introduces the potential for optimizing the control function  $\beta(t)$  to minimize the impact of the epidemic. Specifically, we can aim to reduce the number of infections, control the peak prevalence, and manage the epidemic's duration by adjusting the incidence rate over time. The bounded nature of  $\beta(t)$  ensures that the control remains within realistic limits, avoiding impractical or unsustainable interventions. In our framework, the infection parameter is modeled as  $\beta(t) = p \times c(t)$  where  $c$  represents the average number of contacts per individual and  $p$  denotes the probability of transmission per contact which depends on the virulence of the disease itself. Given that this work aims model potential interventions that are non-pharmaceutical, we adopt the approach outlined in Balderrama et al. [3]. Accordingly, we assume that the time-dependent control function  $\beta$  is constrained between two positive bounds,  $\beta_l$  (the lower bound) and  $\beta_u$  (the upper bound), reflecting the limitations imposed on the contact rate through intervention measures. The remaining parts of the paper are organized as follows. Section 2 is devoted to the paper's primary objective: demonstrat-

ing global controllability of the nonlinear system

$$\begin{cases} \frac{dS(t)}{dt} = -\beta(t)S(t)I(t), \\ \frac{dI(t)}{dt} = \beta(t)S(t)I(t) - \lambda I(t). \end{cases} \quad (3)$$

By analyzing the controllability of this system, we aim to establish a theoretical foundation for designing effective intervention strategies capable of adapting to the evolving dynamics of infectious disease outbreaks. Unlike linear systems, which benefit from a well-established general theory, nonlinear dynamical systems, such as those describing epidemic processes, present significant analytical challenges due to their inherent complexity and lack of universal frameworks. In this context, our study seeks to address these challenges by exploring the controllability of the proposed nonlinear SIR model, with a particular focus on the time-varying incidence rate  $\beta(t)$ . This contribution falls within the framework of full control, which accounts for all variables present in the differential system. In Section 4 of this work, we investigate the concept of partial controllability, specifically focusing on controlling the density of infected individuals,  $I(t)$ , within the population. Partial controllability refers to the ability to influence specific components of a system, in this case, the infected population, without necessarily controlling the entire system. To achieve this, we construct explicit solutions for the system (3). These explicit solutions provide a pathway to control the infected population at any given time during a limited period, offering a practical mechanism for managing the spread of the disease such as reducing the peak of infected individuals or delaying the peak of the epidemic. Furthermore, in Section 5, to address the challenge of epidemic management, we explore numerical methods designed to achieve full control of the SIR system, steering it toward a desired state defined by specific susceptible and infected population levels, denoted as  $(S_d, I_d)$ . These methods utilize an algorithmic approach to iteratively adjust control parameters, ensuring the system converges to the target state effectively. In addition, we propose a hybrid method that combines analytical solutions, derived for partial control scenarios, with an algorithmic framework. This hybrid approach leverages explicit expressions for the time-dependent populations  $S(t)$  and  $I(t)$  to enhance precision, while the algorithmic component optimizes computational efficiency. Together, these techniques offer a practical and adaptable strategy for controlling disease dynamics.

## 2 Well posedness of solutions and their qualitative behavior

In this section, we begin by analyzing the global existence, uniqueness, and boundedness of solutions. Subsequently, we investigate the asymptotic behavior of solutions over long time horizons. To this end, we impose an initial condition  $(S(0), I(0), R(0))$  satisfying

$$S(0) = S_0 > 0, \quad I(0) = I_0 > 0, \quad R(0) = R_0 \geq 0, \quad S_0 + I_0 + R_0 = 1. \quad (4)$$

These conditions ensure a well-posed initial-value problem within the considered epidemic model.

**Theorem 1.** *Assume that  $\beta$  is a continuous function on  $[0, \infty)$ . Then, for any initial condition verifying (4), system (3) admits a unique global solution that is positive and bounded for all  $t \in [0, +\infty)$ .*

*Proof.* Note that system (3) can be equivalently expressed as a non-autonomous Cauchy problem in the

form

$$\begin{cases} y' = \phi(t, y), \\ y(0) = y_0, \end{cases} \quad (5)$$

where

$$y = \begin{pmatrix} x_1 \\ x_2 \end{pmatrix}, \quad \phi(t, y) = \begin{pmatrix} -\beta(t)x_1x_2 \\ \beta(t)x_1x_2 - \lambda x_2 \end{pmatrix}.$$

The function  $f$  is continuous on  $[0, \infty) \times \mathbb{R}_+^2$  and locally Lipschitz with respect to its second variable. Consequently, by the local Picard-Lindelof theorem, differential system (5) admits a unique maximal solution defined on an open interval  $[0, T)$ . Hence, the Kermack-McKendrick model (3) admits a unique solution  $y = (S, I)$  defined on the maximal interval  $[0, T)$ , where  $T > 0$ . An integration of the first and second equations of system (3) gives for all  $t \in [0, T)$

$$S(t) = S_0 \exp\left(-\int_0^t \beta(\tau)I(\tau)d\tau\right) > 0, \quad (6)$$

$$I(t) = I_0 \exp\left(\int_0^t \beta(\tau)S(\tau)d\tau - \lambda t\right) > 0. \quad (7)$$

It follows that

$$\frac{d}{dt}[S(t) + I(t)] = -\lambda I(t) < 0, \quad \forall t \in [0, T).$$

Therefore

$$0 < S(t) + I(t) \leq S_0 + I_0, \quad \forall t \in [0, T).$$

Thus, by virtue of the continuation theorem for ordinary differential equations [16], we conclude that the solution is global. That is  $T = \infty$ .  $\square$

In a second step, it is natural to investigate the asymptotic behavior of the solution  $(S(t), I(t))$  in order to understand the long-term evolution of the epidemic described by the model (3). Specifically, it is necessary to determine sufficient conditions that ensure the extinction of the disease without severe consequences for the population, as well as conditions on the disease parameters that may lead to a major epidemic outbreak. To this end, by virtue of Theorem 1, we have

$$S'(t) = -\beta(t)S(t)I(t) < 0 \quad \forall t \in [0, \infty).$$

Thus,  $S$  is a function which, in addition to being bounded, is strictly decreasing on  $[0, \infty)$ , implying that it admits a finite limit, denoted by  $S_\infty$ , as  $t$  approaches  $\infty$ . We further assert that  $S_\infty > 0$ . By combining the equations governing  $S$  and  $I$  with the positivity of the solutions, we obtain that for all  $t \geq 0$ ,

$$\begin{aligned} \frac{d}{dt}\left(S(t) + I(t) - \frac{\lambda}{\beta_u} \ln(S(t))\right) &= \lambda\left(\frac{\beta(t)}{\beta_u} - 1\right)I(t) \\ &\leq 0. \end{aligned} \quad (8)$$

Consequently, for all  $t \geq 0$ ,

$$S(t) + I(t) - \frac{\lambda}{\beta_u} \ln(S(t)) \leq S_0 + I_0 - \frac{\lambda}{\beta_u} \ln(S_0),$$

which leads to

$$-\frac{\lambda}{\beta_u} \ln(S(t)) \leq S_0 + I_0 - \frac{\lambda}{\beta_u} \ln(S_0), \quad \forall t \geq 0. \quad (9)$$

At this stage, it is evident that  $S_\infty$  is strictly positive. Indeed, if  $S_\infty$  were zero, taking the limit as  $t \rightarrow \infty$  in inequality (9) would lead to a contradiction:

$$\infty \leq S_0 + I_0 - \frac{\lambda}{\beta_u} \ln(S_0).$$

To analyze the asymptotic behavior of  $I(t)$ , we begin by examining the integral equation derived from (6). For all  $t \geq 0$ , it holds that

$$\int_0^t \beta(\tau) I(\tau) d\tau = \ln\left(\frac{S_0}{S(t)}\right).$$

Given that  $\beta(\tau)$  is a positive and bounded function, with a positive lower bound  $\beta_l > 0$ , we can deduce that

$$\int_0^t I(\tau) d\tau \leq \frac{1}{\beta_l} \ln\left(\frac{S_0}{S(t)}\right).$$

Taking the limit superior as  $t \rightarrow \infty$ , and noting that  $S(t)$  converges to a positive value  $S_\infty > 0$ , we obtain

$$\limsup_{t \rightarrow \infty} \int_0^t I(\tau) d\tau \leq \frac{1}{\beta_l} \ln\left(\frac{S_0}{S_\infty}\right).$$

Furthermore, since  $I$  is positive, the improper integral  $\int_0^\infty I(\tau) d\tau$  is convergent. Using  $I$ - equation together with the bounds  $S(t), I(t) \leq 1$  and  $\beta(t) \leq \beta_u$ , we obtain that for all  $t \geq 0$

$$\left| \frac{dI}{dt}(t) \right| \leq \beta_u.$$

By the Mean Value Theorem, we get

$$|I(\tau_1) - I(\tau_2)| \leq \beta_u |\tau_1 - \tau_2|,$$

for all  $\tau_1, \tau_2 \geq 0$ . Hence  $I(t)$  is uniformly continuous on  $[0, \infty)$ . Applying Barbalat's theorem, since all hypotheses are satisfied, we obtain that  $\lim_{t \rightarrow \infty} I(t) = 0$ .

Therefore, the asymptotic results obtained for model (3) can be summarized in the following theorem.

**Theorem 2.** *Assume that  $\beta$  is a continuous positive and bounded function on  $[0, \infty)$ . Then, for any initial condition verifying (4), the solution of model (3) satisfies the following properties:*

$$\lim_{t \rightarrow \infty} S(t) = S(\infty) > 0, \quad \lim_{t \rightarrow \infty} I(t) = 0. \quad (10)$$

### 3 Full controllability of the SIR system by a smooth control

While Theorem 2 guarantees the eventual eradication of the disease, it mainly provides insight into the asymptotic behavior of the epidemic system. However, numerous critical questions concerning the dynamical characteristics of the epidemic remain unresolved. For instance, what is the expected duration



of the epidemic phase? Are there likely to be peaks in the incidence of infections [25], and if so, when are they anticipated to occur, and what magnitude might they attain? Furthermore, are there viable strategies to mitigate or control the spread of the epidemic effectively? In this section, our aim is to address these questions by investigating the full controllability property of the controlled system described in (3). This analysis will provide a deeper understanding of the dynamics of the epidemic and explore potential mechanisms for intervention and control. We still assume that the control class of  $\beta(t)$  is  $\mathcal{C}^0([0, T])$  with  $0 < \beta_l \leq \beta(t) \leq \beta_u < \infty$ .

**Theorem 3.** *Let  $Z_0 = (S_0, I_0)$  in the positive cone of  $\mathbb{R}^2$  with  $S_0 + I_0 \leq 1$ . Then, the reachable set from  $Z_0$  for the controlled system (3) is precisely characterized as follows:*

$$\mathcal{R}_{Z_0} = \{(x, y) \in [0, 1]^2 : x \leq S_0 \text{ and } x + y \leq S_0 + I_0 \leq 1\}. \quad (11)$$

*Proof.* Let  $Z_0 = (S_0, I_0)$  be a point in the positive cone of  $\mathbb{R}^2$ , satisfying  $S_0 + I_0 \leq 1$ . Suppose  $Z_d = (S_d, I_d)$  is a state within the positive cone that is attainable from  $Z_0$  under the dynamics of the controlled system described by system (3). By definition, there exists an admissible control  $\beta$  and a finite time  $\tau \geq 0$  such that the solution  $(S(t), I(t))$  of the system satisfies  $S(\tau) = S_d$  and  $I(\tau) = I_d$ . Using the first equation of (3) and the positivity of  $S$  and  $I$  it is obvious that  $S'(t) < 0$ . That is,  $S(t)$  is a decreasing function. In particular,  $S_d = S(\tau) < S_0$ . By summing the two equations of system (3), the dynamics of the total population  $X(t) = S(t) + I(t)$  are given by  $X'(t) = (S+I)'(t) = -\lambda I(t)$ . Since  $\lambda, I(t) \geq 0$ , it follows that  $X(t) = S(t) + I(t)$  is a decreasing function of time. In particular, at time  $\tau$ , we obtain

$$S_d + I_d = S(\tau) + I(\tau) \leq S(0) + I(0) = S_0 + I_0 \leq 1.$$

Therefore, the reachable set  $\mathcal{R}_{Z_0}$  is contained within the region:

$$\mathcal{R}_{Z_0} \subset \{(x, y) \in [0, 1]^2 : x \leq S_0 \text{ and } x + y \leq S_0 + I_0 \leq 1\}.$$

To establish equality of the reachable set, we now prove the inverse inclusion. Let  $Z_0 = (S_0, I_0)$  be a point in the positive cone of  $\mathbb{R}^2$ , satisfying  $S_0 + I_0 \leq 1$ , and let  $Z_d = (S_d, I_d)$  satisfy:

$$S_d < S_0, \quad S_d + I_d < S_0 + I_0 \quad (12)$$

We aim to construct a positive and a bounded control  $\beta$  that steers the system from  $Z_0$  to  $Z_d$ . For convenience, we reformulate the problem in terms of the state variables  $(X, I)$ . Consequently, the conditions on the initial state  $Z_0$  and the desired state  $Z_d$  given in (12) translate into

$$0 < I_0 < X_0 \leq 1, \quad 0 < I_d < X_d < X_0, \quad (13)$$

where  $X_0 = S_0 + I_0$  and  $X_d = S_d + I_d$ . The construction proceeds by first designing the function  $X(t)$ . Let  $\varepsilon > 0$  be a sufficiently small number, and let  $T > 0$  be a sufficiently large time horizon, both to be determined later. The first step in the construction is to define the function  $X(t)$  on the interval  $[0, T]$  as a  $\mathcal{C}^2$ -smooth function satisfying the following boundary conditions:

$$X(0) = X_0, \quad X'(0) = -\lambda I_0, \quad (14)$$

$$X(T) = X_d, \quad X'(T) = -\lambda I_d. \quad (15)$$

To incorporate the boundary conditions (14) and (15), we define  $X(t)$  piecewise as follows:

$$X(t) = \begin{cases} X_1(t) \triangleq X_0 \exp\left(-\frac{\lambda I_0}{X_0} t\right), & \text{if } t \in [0, \varepsilon], \\ X_2(t), & \text{if } t \in [\varepsilon, T - \varepsilon], \\ X_3(t) \triangleq X_d \exp\left(\frac{\lambda I_d}{X_d} (T - t)\right), & \text{if } t \in [T - \varepsilon, T], \end{cases}$$

where  $X_2(t)$  is a smooth interpolating function to be constructed. The purpose of  $X_2(t)$  is to ensure the global smoothness of  $X(t)$  and to satisfy any additional properties required for the subsequent construction of  $I(t)$ . For instance,  $X$  must be decreasing on  $[0, T]$ . Hence, a necessary condition for this is to have  $X_1(\varepsilon) > X_3(T - \varepsilon)$ , which translates to:

$$X_0 \exp\left(-\frac{\lambda I_0}{X_0} \varepsilon\right) > X_d \exp\left(\frac{\lambda I_d}{X_d} \varepsilon\right).$$

This inequality can be rewritten as:

$$\varepsilon < \frac{\ln(X_0/X_d)}{\lambda \left(\frac{I_0}{X_0} + \frac{I_d}{X_d}\right)}. \quad (16)$$

This condition is feasible since  $X_0 > X_d$  in view of (12). Additionally, we require that  $X' + \lambda X$  is a positive decreasing function of  $[0, T]$ . This property holds on the intervals  $[0, \varepsilon]$  and  $[T - \varepsilon, T]$  as demonstrated by the following expressions:

$$\begin{aligned} X_1'(t) + \lambda X_1(t) &= \lambda(X_0 - I_0) \exp\left(-\frac{\lambda I_0}{X_0} t\right) & \forall t \in [0, \varepsilon], \\ X_3'(t) + \lambda X_3(t) &= \lambda(X_d - I_d) \exp\left(\frac{\lambda I_d}{X_d} (T - t)\right) & \forall t \in [\varepsilon, T - \varepsilon]. \end{aligned}$$

We will construct  $X_2$  to maintain these properties on  $[\varepsilon, T - \varepsilon]$ . To this end, we define the following quantities at the transition points  $t = \varepsilon$  and  $t = T - \varepsilon$ :

$$\begin{aligned} K_{11}^\varepsilon &\triangleq X_1'(\varepsilon) + \lambda X_1(\varepsilon) = \lambda(X_0 - I_0) \exp\left(-\frac{\lambda I_0}{X_0} \varepsilon\right), \\ K_{12}^\varepsilon &\triangleq -[X_1''(\varepsilon) + \lambda X_1'(\varepsilon)] = \frac{\lambda^2 I_0}{X_0} (X_0 - I_0) \exp\left(-\frac{\lambda I_0}{X_0} \varepsilon\right), \end{aligned}$$

and

$$\begin{aligned} K_{21}^\varepsilon &\triangleq X_3'(T - \varepsilon) + \lambda X_3(T - \varepsilon) = \lambda(X_d - I_d) \exp\left(\frac{\lambda I_d}{X_d} \varepsilon\right), \\ K_{22}^\varepsilon &\triangleq -[X_3''(T - \varepsilon) + \lambda X_3'(T - \varepsilon)] = \frac{\lambda^2 I_d}{X_d} (X_d - I_d) \exp\left(\frac{\lambda I_d}{X_d} \varepsilon\right). \end{aligned}$$

Note that

$$\frac{K_{12}^\varepsilon}{K_{11}^\varepsilon} = \frac{\lambda I_0}{X_0} < \lambda, \quad \frac{K_{22}^\varepsilon}{K_{21}^\varepsilon} = \frac{\lambda I_d}{X_d} < \lambda.$$



To ensure  $X \in \mathcal{C}^2([0, T])$ , we solve the differential equation:

$$X_2'(t) + \lambda X_2(t) = f(t), \quad (17)$$

where  $f(t)$  is a positive, decreasing function satisfying

$$f(\varepsilon) = K_{11}^\varepsilon, \quad f'(\varepsilon) = -K_{12}^\varepsilon, \quad (18)$$

$$f(T - \varepsilon) = K_{21}^\varepsilon, \quad f'(T - \varepsilon) = -K_{22}^\varepsilon. \quad (19)$$

We define  $f(t)$  piecewise as

$$f(t) = \begin{cases} K_{11}^\varepsilon \exp\left(-\frac{\lambda I_0}{X_0}(t - \varepsilon)\right), & t \in [\varepsilon, 2\varepsilon], \\ K_{11}^\varepsilon \exp\left(-\frac{\lambda I_0 \varepsilon}{X_0}\right) \exp(-a(t - 2\varepsilon)), & t \in [2\varepsilon, T - 2\varepsilon], \\ K_{21}^\varepsilon \exp\left(\frac{\lambda I_d}{X_d}(T - \varepsilon - t)\right), & t \in [T - 2\varepsilon, T - \varepsilon], \end{cases} \quad (20)$$

where  $a$  satisfies

$$\exp(-a(T - 4\varepsilon)) = \frac{X_d - I_d}{X_0 - I_0} \cdot \exp\left(2\lambda \left(\frac{I_0}{X_0} + \frac{I_d}{X_d}\right) \varepsilon\right). \quad (21)$$

to insure the continuity of  $f$  on the interval  $[\varepsilon, T - \varepsilon]$ . This is possible because given that  $\frac{X_0 - I_0}{X_d - I_d} > 1$ , one can chose  $\varepsilon$  small enough to verify

$$\exp\left(2\lambda \left(\frac{I_0}{X_0} + \frac{I_d}{X_d}\right) \varepsilon\right) < \frac{X_0 - I_0}{X_d - I_d}. \quad (22)$$

Furthermore, the aforementioned condition is equivalent to  $f(2\varepsilon) > f(T - 2\varepsilon)$ , which is consistent with the requirement that  $f$  be a decreasing function. The following two inequalities will be used later in this proof, both depending on the parameter  $\varepsilon$ . The first inequality holds with a negative value for all  $\varepsilon$ . For the second inequality, we choose  $\varepsilon$  sufficiently small to ensure that it holds with a positive value:

$$\begin{aligned} L_1(\varepsilon) &= -X_d \exp\left(\lambda \varepsilon \left(\frac{2I_d}{X_d} - 1\right)\right) < 0, \\ L_2(\varepsilon) &= X_d \exp\left(-\lambda \varepsilon + 2\frac{\lambda I_d}{X_d} \varepsilon\right) \left(\frac{X_0}{X_d} \exp\left(-2\lambda \varepsilon \left(\frac{I_0}{X_0} + \frac{I_d}{X_d}\right)\right) - 1\right) > 0. \end{aligned}$$

Using the integral representation of  $X_2(t)$ , we write

$$X_2(t) = X_1(\varepsilon) \exp(-\lambda(t - \varepsilon)) + \int_\varepsilon^t \exp(-\lambda(t - u)) f(u) du. \quad (23)$$

Combining (17), (18) and (19), we get

$$X_2(\varepsilon) = X_1(\varepsilon), \quad X_2'(\varepsilon) = X_1'(\varepsilon), \quad X_2''(\varepsilon) = X_1''(\varepsilon).$$

These equalities ensure that the function  $X$  is of class  $\mathcal{C}^2$  on the interval  $[0, T - \varepsilon]$ . Finally, to guarantee

the regularity of  $X$  at  $t = T - \varepsilon$ , we analyze the zeros of the equation

$$F_\varepsilon(a) \triangleq X_2(T - \varepsilon) - X_3(T - \varepsilon) = 0,$$

which implicitly determines  $a$ , and so  $T$ . We will use the Intermediate Value Theorem to prove that the function  $F_\varepsilon$  admits a root on  $(0, \infty)$ . As a direct result of previous relations we have

$$F_\varepsilon(a) = X_0 \exp(-\lambda T - 2\lambda \varepsilon \frac{I_0}{X_0}) + A_{1\varepsilon}(a) + A_{2\varepsilon}(a) + A_{3\varepsilon}(a) - X_d \exp\left(\frac{\lambda I_d}{X_d} \varepsilon\right), \quad (24)$$

where

$$\begin{aligned} A_{1\varepsilon}(a) &= \int_\varepsilon^{2\varepsilon} \exp(-\lambda(T - \varepsilon - u)) K_{11}^\varepsilon \exp\left(-\frac{\lambda I_0}{X_0}(u - \varepsilon)\right) du \\ &= \frac{K_{11}^\varepsilon}{\lambda \left(1 - \frac{I_0}{X_0}\right)} \exp\left(-\lambda T + \lambda \varepsilon + \frac{\lambda I_0}{X_0} \varepsilon\right) \left[ \exp\left(2\lambda \varepsilon \left(1 - \frac{I_0}{X_0}\right)\right) \right. \\ &\quad \left. - \exp\left(\lambda \varepsilon \left(1 - \frac{I_0}{X_0}\right)\right) \right], \end{aligned} \quad (25)$$

$$\begin{aligned} A_{2\varepsilon}(a) &= \int_{2\varepsilon}^{T-2\varepsilon} \exp(-\lambda(T - \varepsilon - u)) K_{11}^\varepsilon \exp\left(-\frac{\lambda \varepsilon I_0}{X_0}\right) \exp(-a(u - 2\varepsilon)) du \\ &= \frac{K_{11}^\varepsilon}{\lambda - a} \exp\left(-\frac{\lambda I_0 \varepsilon}{X_0}\right) \exp(-\lambda T + \lambda \varepsilon + 2a\varepsilon) [\exp((\lambda - a)(T - 2\varepsilon)) \\ &\quad - \exp((\lambda - a)(2\varepsilon))], \end{aligned} \quad (26)$$

$$\begin{aligned} A_{3\varepsilon}(a) &= \int_{T-2\varepsilon}^{T-\varepsilon} \exp(-\lambda(T - \varepsilon - u)) K_{21}^\varepsilon \exp\left(\frac{\lambda I_d}{X_d}(T - \varepsilon - u)\right) du \\ &= \frac{K_{21}^\varepsilon}{\lambda \left(1 - \frac{\lambda I_d}{X_d}\right)} \left[ 1 - \exp\left(-\lambda \varepsilon \left(1 - \frac{I_d}{X_d}\right)\right) \right]. \end{aligned} \quad (27)$$

From (21), it follows that as  $a \rightarrow 0^+$ ,  $T \rightarrow \infty$  and as  $a \rightarrow \infty$ ,  $T \rightarrow 4\varepsilon$ . Hence, combining (24), (25), (26) and (27), we obtain that

$$\lim_{a \rightarrow 0^+} F_\varepsilon(a) = L_1(\varepsilon) < 0 \quad \text{and} \quad \lim_{a \rightarrow \infty} F_\varepsilon(a) = L_2(\varepsilon) > 0. \quad (28)$$

Furthermore, one should not omit the particular case when  $a \rightarrow \lambda$  in the term  $A_{2\varepsilon}$ , because it could corrupt the continuity of  $F$ . Despite that  $\lambda$  is a singularity of  $A_{2\varepsilon}$  its limit is finite and thus admits a continuous extension. This result is simply obtained by the application of L'Hôpital's rule on the function

$$a \mapsto \frac{\exp((\lambda - a)(T - 2\varepsilon)) - \exp((\lambda - a)(2\varepsilon))}{\lambda - a}.$$

Using (28) and the fact the  $F_\varepsilon$  is a continuous function, we conclude that there exists a positive  $a$  that

verifies  $F_\varepsilon(a) = 0$  by means of the Intermediate Value Theorem. In other words, there exists  $T > 4\varepsilon$  such that  $X_2(T - \varepsilon) = X_3(T - \varepsilon)$ , which also gives according to (23), (18) and (19) that

$$X_2'(T - \varepsilon) = X_3'(T - \varepsilon), \quad X_3''(T - \varepsilon) = X_2''(T - \varepsilon).$$

Thus,  $X$  is a  $\mathcal{C}^2$  function on  $[0, T]$ . Next, we put

$$I(t) = -\frac{1}{\lambda}X'(t), \quad \forall t \in [0, T].$$

Then according to (14) and (15), the function  $I(t)$  satisfies both the initial and terminal conditions:

$$I(0) = I, \quad I(T) = I_d.$$

Furthermore, leveraging the positivity of  $f(t)$ , we observe that

$$I(t) = -\frac{1}{\lambda}X'(t) = -\frac{1}{\lambda}(-\lambda X(t) + f(t)) < X(t). \quad (29)$$

Additionally,  $X(t)$  remains strictly decreasing on  $[0, T]$ . To establish this, note that  $X(t)$  is initially decreasing and convex on  $[0, \varepsilon]$  and ultimately decreasing on  $[T - \varepsilon, T]$ . If  $X(t)$  were to lose its monotonicity at some intermediate time  $\tau \in (\varepsilon, T - \varepsilon)$ , then  $X'(\tau) = 0$  and  $X(t)$  would need to exhibit local convexity near  $\tau$ . However, in such a case, we compute

$$X''(\tau) = f'(\tau) - \lambda X'(\tau) = f'(\tau) < 0,$$

which is negative due to the decreasing nature of  $f(t)$ . This contradicts the assumption of convexity. Hence,  $X(t)$  is strictly decreasing on  $[0, T]$ , and consequently

$$I(t) = -\frac{1}{\lambda}X'(t) > 0 \quad \forall t \in [0, T]. \quad (30)$$

Next, we proceed to determine the form of the control  $\beta(t)$  that steers the system from an initial state  $(S_0, I_0)$  to a desired terminal state  $(S_d, I_d)$ . To this end, we define  $\beta(t)$  as

$$\beta(t) = \frac{I'(t) + \lambda I(t)}{(X(t) - I(t))I(t)}.$$

Since  $\beta(t)$  is a continuous function on the compact interval  $[0, T]$ , it is necessarily bounded. Moreover, combining inequalities (29) and (30) with the fact that  $f(t)$  is constructed to be decreasing, we deduce that

$$\beta(t) = \frac{-X''(t)/\lambda + X(t)}{(X(t) - I(t))I(t)} > 0.$$

Thus,  $\beta(t)$  is an admissible control that successfully drives system (3) from the initial state  $Z_0$  to the desired terminal state  $Z_d$ .  $\square$

## 4 Partial controllability of infected population

The analysis presented in the preceding section shows the theoretical feasibility of guiding the state of the epidemic system from an initial condition, denoted as,  $Z_0$ , to any prescribed state within the reachable set  $\mathcal{R}_{Z_0}$  within a finite temporal horizon. This result underscores the potential efficacy of targeted interventions in modulating the trajectory of the epidemic system. However, a critical limitation emerges from the implicit characterization of the temporal duration required to achieve the desired state, as this duration may be excessively prolonged, particularly in practical scenarios where rapid and timely intervention is essential to mitigate the spread of infection and minimize its impact on the population. This constraint significantly reduces the practical utility of such control strategies, especially in emergency or high-stakes situations where immediate action is paramount. To address these limitations, in this section, we build on the methodological framework established in [9, 27], which focuses on the implementation of a partial control strategy to regulate the number of infected individuals within a population. While the cited works provide a foundational approach to managing the spread of infection through targeted interventions, our study extends this paradigm by proposing a dual-control framework. This framework introduces two distinct yet complementary control mechanisms, each designed to address specific aspects of infection dynamics. The first control mechanism is characterized by a single-peak intervention strategy. This approach involves a concentrated and time-limited effort to reduce the number of infectives at a critical point in the epidemic trajectory. This strategy is particularly effective in scenarios where immediate action is required to mitigate a sudden surge in infections, thus preventing the system from reaching a tipping point that could lead to uncontrolled spread. The second control mechanism aligns with the methodologies described in [9, 27], focusing on a sustained and systematic approach to infection control. This mechanism is designed to achieve an exponential decay in the density of infected individuals over time. By continuously applying this control, the population gradually moves toward a state of reduced infection prevalence, ensuring long-term stability and minimizing the risk of recurrent outbreaks. The integration of these two control strategies—one focused on short-term, high-intensity intervention and the other on long-term, sustained suppression—provides a comprehensive approach to managing infectious disease dynamics. This dual-control framework not only addresses the immediate challenges posed by sudden increases in infection rates but also ensures a robust and enduring reduction in the overall burden of disease within the population. Through this approach, we aim to contribute a more nuanced and effective strategy for epidemic control, building upon the foundational work of the referenced studies while introducing innovative elements to enhance their applicability and impact.

Let us assume that  $\mathcal{R}_0 > 1$ . Then, at the onset of the epidemic, the density of infected individuals increases exponentially, following an approximate law of the form

$$I(t) \approx I_0 \exp[(\beta(0)S_0 - \lambda)t],$$

which gives rise to an initial peak. However, variability in the transmission rate may induce successive peaks in the epidemic curve. Moreover, the asymptotic behavior of  $I(t)$  is characterized by an exponential decline, indicating a rapid reduction in the number of cases proportional to the infected population until the eventual extinction of the disease. However, this decline is not uniform over the entire interval. In this section, we aim to determine an instantaneous control  $\beta(t)$  such that  $I(t)$  can be expressed as a linear combination of two exponentially decreasing functions. Let  $a > 1$  and  $b_1, b_2 > 0$ . We seek an admissible

solution to system (3) of the form

$$I_{a,b_1,b_2}(t) = I_0 \left( ae^{-b_1 t} - (a-1)e^{-b_2 t} \right). \quad (31)$$

In this configuration, the choice of the controlled transmission rate  $\beta(t)$  is closely related to the configuration of the parameters  $a, b_1$ , and  $b_2$ . Since we have assumed that  $\mathcal{R}_0 > 1$ , an admissible solution  $I_{a,b_1,b_2}(t)$  must initially increase. Taking into account expression (31), this initial condition translates into the inequality

$$(a-1)b_2 - ab_1 > 0. \quad (32)$$

To determine the optimal control  $\beta(t)$  leading to the desired infected density (31), we first compute the susceptible density by solving the differential equation

$$S'(t) = -I'_{a,b_1,b_2}(t) - \lambda I_{a,b_1,b_2}(t).$$

This yields the following expression:

$$S_{a,b_1,b_2}(t) = S_0 + I_0 - I_{a,b_1,b_2}(t) - \lambda \int_0^t I_{a,b_1,b_2}(\tau) d\tau \quad \forall t \geq 0. \quad (33)$$

Substituting (31), we obtain

$$S_{a,b_1,b_2}(t) = S_0 + I_0 - \lambda I_0 \left( \frac{a}{b_1} - \frac{a-1}{b_2} \right) + I_0 \left( \frac{a(\lambda - b_1)}{b_1} e^{-b_1 t} - \frac{(a-1)(\lambda - b_2)}{b_2} e^{-b_2 t} \right). \quad (34)$$

To ensure that  $S_{a,b_1,b_2}(t)$  is an admissible solution to system (3), we must verify whether it is a decreasing and positive function. We compute its derivative, which is

$$S'_{a,b_1,b_2}(t) = I_0 e^{-b_1 t} \left[ (a-1)(\lambda - b_2) e^{-(b_2 - b_1)t} - a(\lambda - b_1) \right].$$

The condition (32) ensures that  $b_2 > b_1$ . Thus, for  $S_{a,b_1,b_2}(t)$  to be decreasing, we choose  $b_1$  and  $b_2$  such that

$$\begin{aligned} \lambda - b_2 \leq 0, \quad (a-1)(\lambda - b_2) - a(\lambda - b_1) < 0, \quad -a(\lambda - b_1) < 0, \\ \text{or} \\ \lambda - b_2 > 0, \quad (a-1)(\lambda - b_2) - a(\lambda - b_1) < 0. \end{aligned}$$

That is,  $b_1$  and  $b_2$  satisfy the conditions

$$(b_1 < \lambda \leq b_2, \quad ab_1 - (a-1)b_2 < \lambda) \text{ or } (b_2 < \lambda, \quad ab_1 - (a-1)b_2 < \lambda).$$

In view of condition (32), this is equivalent to

$$b_1 < \lambda \leq b_2, \quad \text{or} \quad b_2 < \lambda. \quad (35)$$

To guarantee the positivity of  $S_{a,b_1,b_2}(t)$ , we compute its asymptotic limit as follows:

$$S_{a,b_1,b_2}(\infty) = S_0 + I_0 - \lambda I_0 \left( \frac{a}{b_1} - \frac{a-1}{b_2} \right).$$

Given the monotonicity of  $S_{a,b_1,b_2}(t)$ , ensured by condition (4), its positivity requires

$$\frac{a}{b_1} - \frac{a-1}{b_2} < \frac{S_0 + I_0}{\lambda I_0}. \quad (36)$$

We can now define the candidate control  $\beta_{a,b_1,b_2}(t)$  as follows:

$$\begin{aligned} \beta_{a,b_1,b_2}(t) &= \frac{-S'_{a,b_1,b_2}(t)}{S_{a,b_1,b_2}(t)I_{a,b_1,b_2}(t)} \\ &= \frac{a(\lambda - b_1) - (a-1)(\lambda - b_2)e^{-(b_2-b_1)t}}{\left[ S_0 + I_0 - \lambda I_0 \left( \frac{a}{b_1} - \frac{a-1}{b_2} \right) + I_0 \left( \frac{a(\lambda - b_1)}{b_1} e^{-b_1 t} - \frac{(a-1)(\lambda - b_2)}{b_2} e^{-b_2 t} \right) \right] [a - (a-1)e^{-(b_2-b_1)t}]}. \end{aligned}$$

Given the conditions (32), (35) and (36), the function  $-S'_{a,b_1,b_2}$ ,  $S_{a,b_1,b_2}$  and  $I_{a,b_1,b_2}$  are positive, then  $\beta_{a,b_1,b_2}$  is positive on  $[0, \infty)$ . Furthermore, it is continuous on  $[0, \infty)$  with finite limit at infinity given by

$$\beta_{a,b_1,b_2}(\infty) = \frac{\lambda - b_1}{S_0 + I_0 - \lambda I_0 \left( \frac{a}{b_1} - \frac{a-1}{b_2} \right)}.$$

Thus,  $\beta_{a,b_1,b_2}$  is also bounded on  $[0, \infty)$ . It follows from (33) and (4) that the pair  $(S_{a,b_1,b_2}(t), I_{a,b_1,b_2}(t))$  is a solution to system (3) when the transmission rate is given by  $\beta_{a,b_1,b_2}(t)$ . The following theorem summarizes the preceding findings.

**Theorem 4.** *For the initial condition  $(S_0, I_0)$ , if the following conditions hold*

$$\begin{cases} a > 1, & b_2, b_1 > 0, \\ (a-1)b_2 - ab_1 > 0, \\ b_1 < \lambda \leq b_2, & \text{or } b_2 < \lambda, \\ \frac{a}{b_1} - \frac{a-1}{b_2} < \frac{S_0 + I_0}{\lambda I_0}, \end{cases}$$

*then the control  $\beta_{a,b_1,b_2}(t)$  given by (4) is admissible, and the associated solution to system (3) is given by the explicit expressions (34) and (31).*

Assume now that  $\mathcal{R}_0 \leq 1$ . Under this condition, the density of infected individuals decreases at the onset of the epidemic. To sustain this decline and ensure it follows an exponential trajectory, our objective is to determine an instantaneous control function  $\beta(t)$  such that  $I(t)$  can be represented as an exponentially decreasing function. Specifically, for a given constant  $c > 0$ , we seek an admissible solution to system (3) of the form

$$I_c(t) = I_0 e^{-ct}. \quad (37)$$

Following the methodology used in the case where  $\mathcal{R}_0 > 1$ , we derive the corresponding expression for

the density of susceptible individuals  $S_c(t)$ . This yields

$$S_c(t) = S_0 - \frac{(\lambda - c)I_0}{c} + \frac{(\lambda - c)I_0}{c} e^{-ct}. \quad (38)$$

To ensure the positivity and the decreasing nature of  $S_c(t)$ , the parameter  $c$  must satisfy the following inequality:

$$0 < \frac{(\lambda - c)I_0}{c} < S_0.$$

This condition can equivalently be expressed as

$$\frac{\lambda I_0}{S_0 + I_0} < c < \lambda. \quad (39)$$

The controlled transmission rate  $\beta_c(t)$  is defined via the relation

$$\beta_c(t) = \frac{-S'_c(t)}{S_c(t)I_c(t)}. \quad (40)$$

Substituting the expressions for  $S'_c(t)$ ,  $S_c(t)$ , and  $I_c(t)$  into (40), we obtain the following explicit form for  $\beta_c(t)$

$$\beta_c(t) = \frac{\lambda - c}{S_0 - \frac{(\lambda - c)I_0}{c} + \frac{(\lambda - c)I_0}{c} e^{-ct}}. \quad (41)$$

Under the conditions specified in (39), the function  $\beta_c(t)$  is positive, bounded, and well-defined for all  $t \geq 0$ . We summarize the findings in the following theorem.

**Theorem 5.** *For the initial condition  $(S_0, I_0)$ , let condition (39) hold. Then, the control  $\beta_c(t)$  given by (41) is admissible, and the associated solution to system (3) is given by the explicit expressions (38) and (37).*

## 5 An algorithmic approach to reach full control

The high precision of the analytical methods discussed earlier provides an excellent framework to guide the system toward the desired destination point. However, as demonstrated with the full control approach outlined in Section 3, deriving an explicit form proves challenging, necessitating reliance on numerical methods to address the integral equations that emerge during solution construction. Consequently, this section introduces algorithmic strategies designed to achieve  $Z_d$ . Notably, the algorithmic approaches presented here do not yield an exact solution but establish an iterative process that converges toward the precise destination point.

The initial algorithm employed, inspired by dichotomous search, leverages numerical continuation and parameter sweeps, entailing the resolution of the ordinary differential equation (ODE) system across a spectrum of  $\beta$  values. The function  $\phi$  in system (3) satisfies the essential conditions for numerical continuation, namely Lipschitz continuity, uniform boundedness, and continuous dependence of both the equations and initial conditions on the parameters  $\beta$  and  $\lambda$ . These algorithms operate by fixing the initial condition  $Z_0$  and the parameter  $\lambda$ , designating  $\beta$  as the sole variable parameter. To this end, we



initially assume that  $Z_d$  fulfills the reachability conditions.

The first algorithm introduced adopts a dichotomous approach, presupposing that  $Z_d$  can be attained using a constant positive  $\beta$  value. The critical initial step of this algorithm hinges on identifying two suitable  $\beta$  values to commence the process. Specifically, the criteria for selecting these values, denoted  $\beta_0$  and  $\beta_1$ , ensure the existence of  $T_0, T_1 \in (0, \infty)$  such that  $S_{\beta_0}(T_0) = S_d$  and  $I_{\beta_0}(T_0) < I_d$ , and  $S_{\beta_1}(T_1) = S_d$  and  $I_{\beta_1}(T_1) > I_d$ , where  $T_0$  and  $T_1$  are respectively dependent on  $\beta_0$  and  $\beta_1$ . By drawing on insights from the concluding paragraph of Section 3, we can readily determine appropriate values for  $\beta_0$  and  $\beta_1$ . Once initialized, and akin to a classical dichotomy method, we construct a sequence  $\{\beta_n\}$ , as elaborated in the subsequent pseudo-Algorithm. Note that the ODE\_SOLVER employed here is a classical method based on the Euler scheme. To avoid unnecessary computation, the solver terminates as soon as a time  $\tau$  is reached such that  $S(\tau) \geq S_d$ . This stopping criterion justifies the inclusion of  $S_d$  as an argument of the ODE\_SOLVER function. In the pseudo-Algorithm given,  $T_a$  and  $T_b$  are stopping times for solutions generated with  $\beta_a$  and  $\beta_b$  consecutively. The second algorithm employs a Monte Carlo-based approach. Our initial implementation is straightforward: it conducts multiple trials by sampling values of the parameter  $\beta$  from a normal distribution centered on the true value, then simulates the corresponding trajectories  $(S_t, I_t)$ . Among these, we select the trajectory that terminates closest to the target point  $(S_d, I_d)$  at the final time  $t = T$ . The algorithm terminates once a sufficiently accurate solution is found. However, this reliance on random sampling for  $\beta$  proves computationally inefficient. Rather than employing iterative refinement or gradient-based optimization, the algorithm depends on stochastic guesses, leading to excessive computational cost as the probability of selecting an optimal  $\beta$  decreases rapidly with increasing problem complexity. The variance inherent in the normal distribution exacerbates this issue, as even small deviations in  $\beta$  can result in significant trajectory errors, particularly in systems sensitive to parameter perturbations. Furthermore, the absence of visualization for intermediate results obscures insights into the algorithm's performance, making it difficult to diagnose issues with convergence or adaptability. Consequently, this brute-force approach is poorly suited for this problem. That is why, based on this poor performance we quickly quit this approach and looked for alternatives. One of the efficient methods we've found is inspired from CMA-ES algorithm that was presented years ago [14, 15] but still outperformed global search methods consistently as reported recently by Ozaki et al [23]. This method adopts a more structured exploration of the parameter space. Instead of relying solely on random sampling, we generate a collection of  $m$  candidate  $\beta$ -values either (i) via uniform random sampling within a prescribed interval or (ii) as uniformly spaced values  $\beta_0, \beta_1, \dots$  across the same interval. From these candidates, we select the optimal  $\beta$  that minimizes the distance  $|I_T - I_d|$ , based on an argmin criterion. The second-best candidate is then selected from the remaining  $m - 1$  values, further refining the parameter choice. The pseudo-Algorithm 1 explains how to achieve the previous process.

As evident from the previous pseudo-Algorithm, we employed a function named CANDIDATE, which identifies the optimal pair of beta values and returns them along with the final two values of their corresponding solutions.

To evaluate the performance of the algorithms in approximating the parameter  $\beta$ , a synthetic benchmark was constructed. Specifically, a reference trajectory was first generated using a predetermined exact value of  $\beta_{ex}$ . From this trajectory, a destination point  $(S_d^{\beta_{ex}}, I_d^{\beta_{ex}})$  was selected at random. This known final state, together with the system dynamics, was then used as a target for the inverse problem: estimating the value of  $\beta$  that would reproduce the given endpoint. Consequently, while the algorithms operate under the assumption of an unknown  $\beta$ , the true value is known a priori, allowing for a direct and quantitative assessment of the accuracy and efficiency of each method. Table 1 compares the performance

**Algorithm 1 : Dichotomy of  $\beta$  Values**


---

```

1: Require:  $S_0, I_0, S_d, I_d > 0, S_0 \geq S_d$  and  $S_0 + I_0 \geq S_d + I_d$ 
2: Initialize:  $\beta_a \leftarrow \beta_0, \beta_b \leftarrow \beta_1, \beta'_a \leftarrow \beta_0, \beta'_b \leftarrow \beta_1, it \leftarrow 1, \varepsilon \ll \text{err}, N_{\max}$ 
3: while  $\text{err} > \varepsilon$  and  $it < N_{\max}$  do
4:    $\beta'_a \leftarrow \beta_a, \beta'_b \leftarrow \beta_b$  {Store old value before update}
5:    $(S_a(t), I_a(t)) \leftarrow \text{ODE\_SOLVER}(S_0, I_0, \beta'_a, \lambda, T_{\max}, dt, S_d)$ 
6:    $(S_b(t), I_b(t)) \leftarrow \text{ODE\_SOLVER}(S_0, I_0, \beta'_b, \lambda, T_{\max}, dt, S_d)$ 
7:    $\text{err}_a \leftarrow I_a(T_a) - I_d, \text{err}_b \leftarrow I_b(T_b) - I_d, \text{err} \leftarrow \sqrt{\text{err}_a^2 + \text{err}_b^2}$ 
8:   if  $|\text{err}_a| < |\text{err}_b|$  then
9:     if  $\text{err}_a < 0$  then
10:      if  $\text{err}_b > 0$  then
11:         $\beta_b \leftarrow (\beta_a + \beta_b)/2$  {Bisection update}
12:      else
13:         $\beta_b \leftarrow \beta'_b$  {Revert to old value if needed}
14:      end if
15:    else
16:       $\beta_b \leftarrow \beta_a, \beta_a \leftarrow \beta'_a$  {Revert to old value}
17:    end if
18:  else
19:    if  $\text{err}_b > 0$  then
20:      if  $\text{err}_a < 0$  then
21:         $\beta_a \leftarrow (\beta_a + \beta_b)/2$  {Bisection update}
22:      else
23:         $\beta_a \leftarrow \beta'_a$  {Revert to old value}
24:      end if
25:    else
26:       $\beta_a \leftarrow \beta_b, \beta_b \leftarrow \beta'_b$  {Revert to old value}
27:    end if
28:  end if
29:   $it \leftarrow it + 1$ 
30: end while

```

---

**Algorithm 2 : Monte Carlo  $\beta$** 


---

```

1: Require:  $S_0, I_0, S_d, I_d > 0, S_0 \geq S_d$  and  $S_0 + I_0 \geq S_d + I_d$ 
2: Initialize:  $it \leftarrow 1, \varepsilon \ll \text{errI}$  and  $N_{\max}$ .
3: while  $k < N_{\max}$  and  $\text{errI}_1 > \varepsilon$  and  $\text{errI}_2 > \varepsilon$  do
4:    $\beta_{11}, \beta_{12}, I'_{11}, I'_{12} \leftarrow \text{CANDIDATE}(\beta_1, m, \rho, S_d, I_d, S_0, I_0, T_{\max}, dt, \lambda)$ 
5:    $\beta_{11}, \beta_{12}, I'_{11}, I'_{12} \leftarrow \text{CANDIDATE}(\beta_1, m, \rho, S_d, I_d, S_0, I_0, T_{\max}, dt, \lambda)$ 
6:   if  $I'_{11} < I'_{21}$  then
7:      $\beta_1, \beta_2 \leftarrow \beta_{11}, \beta_{12}$ 
8:      $I_1, I_2 \leftarrow I'_{21}, I'_{22}$ 
9:   end if
10:   $\rho \leftarrow |\beta_1 - \beta_2|$ 
11:   $\text{errI}_1, \text{errI}_2 \leftarrow |I_1 - I_d|, |I_2 - I_d|$ 
12: end while
13: Output:  $\hat{\beta}$  the best estimation found.

```

---

of the two different Algorithms 1 and 2 by listing, for various precision levels, the number of iterations required, the corresponding approximate values of  $\beta$  and also the execution time of each one.

To numerically exploit the analysis presented in Section 4, we intend to complement the theoretical framework of partial control with an algorithm that, in certain instances, enables full control of the disease by guiding the system to a desired state  $(S_d, I_d)$ . Specifically, based on equation (31), to determine

**Algorithm 3** : Candidate

---

```

1: Require:  $\beta_0, m, \rho, S_d, I_d, S_0, I_0, T_{max}, dt, \lambda$ 
2: if  $\beta_0 \leq \rho$  then
3:    $TAB_\beta \leftarrow$  Generate  $m$  values for  $\beta$  in the interval  $[0, \beta_0 + \rho]$ .
4: else
5:    $TAB_\beta \leftarrow$  Generate  $m$  values for  $\beta$  in the interval  $[\beta_0 - \rho, \beta_0 + \rho]$ 
6: end if
7: for  $\beta_k \in TAB_\beta$  do
8:    $I_k \leftarrow \text{ODE\_SOLVER}(S_0, I_0, \beta_k, \lambda, T_{max}, dt, S_d)$ 
9:   Store the error between the last value of  $I_k$  and  $I_d$ 
10: end for
11: Select the two best values (minimal error) among the  $m$  values of  $TAB_\beta$ 
12: OUTPUT:  $\beta_1, \beta_2, I_1^{last}, I_2^{last}$ 

```

---

a time  $T$  at which  $I_{a,b_1,b_2}(T) = I_d$ , the following equation must be satisfied:

$$I_0 \left( ae^{-b_1 T} - (a-1)e^{-b_2 T} \right) = I_d,$$

which can be transformed into a transcendental equation by defining  $\tau = e^T$ , yielding:

$$\frac{a}{\tau^{b_1}} - \frac{a-1}{\tau^{b_2}} = \frac{I_d}{I_0}. \quad (42)$$

**Table 1:** Comparison of precision, number of iterations, and approximate values of  $\beta$  across different algorithms and execution time. The exact value of  $\beta$  is 0.12 .

	Precision	Iterations	$\beta_{inf}$	$\beta_{sup}$	Exec. Time (s)
<b>Dichotomy</b>	$10^{-4}$	2	0.11999971068	0.12000003814	0.41
<b>Montecarlo 2</b>		3	0.11999971068	0.12000092886	10.86
<b>Dichotomy</b>	$10^{-6}$	20	0.11999969482	0.12000038146	0.31
<b>Montecarlo 2</b>		3	0.11999971068	0.12000092886	10.75
<b>Dichotomy</b>	$10^{-8}$	24	0.11999999523	0.12000038146	0.38
<b>Montecarlo 2</b>		4	0.11999999839	0.12000001063	17.08
<b>Dichotomy</b>	$10^{-10}$	31	0.11999999992	0.12000000026	0.46
<b>Montecarlo 2</b>		5	0.11999999999	0.12000000011	22.00

Our approach then involves identifying an optimal combination of parameters  $a$ ,  $b_1$ , and  $b_2$  to minimize the deviation of  $S(T)$  from  $S_d$  when  $I(T) = I_d$ . This numerical strategy is designed for scenarios where the initial reproductive number  $\mathcal{R}_0 > 1$ . As elucidated in Section 4, the explicit expression for  $S(t)$  is derived from that of  $I(t)$ , implying that while reaching a specific value of  $I$  (i.e.,  $I_d$ ) is assured, the corresponding  $S(T)$  is not uniquely fixed. Fortunately, the non-uniqueness of  $a$ ,  $b_1$ , and  $b_2$  permits exploration across the feasible region to identify parameter values that align  $S(T)$  closely with  $S_d$  when  $I(T) = I_d$ .

The delineation of the feasible region is detailed in Algorithm 4. Accordingly, the initial step consists

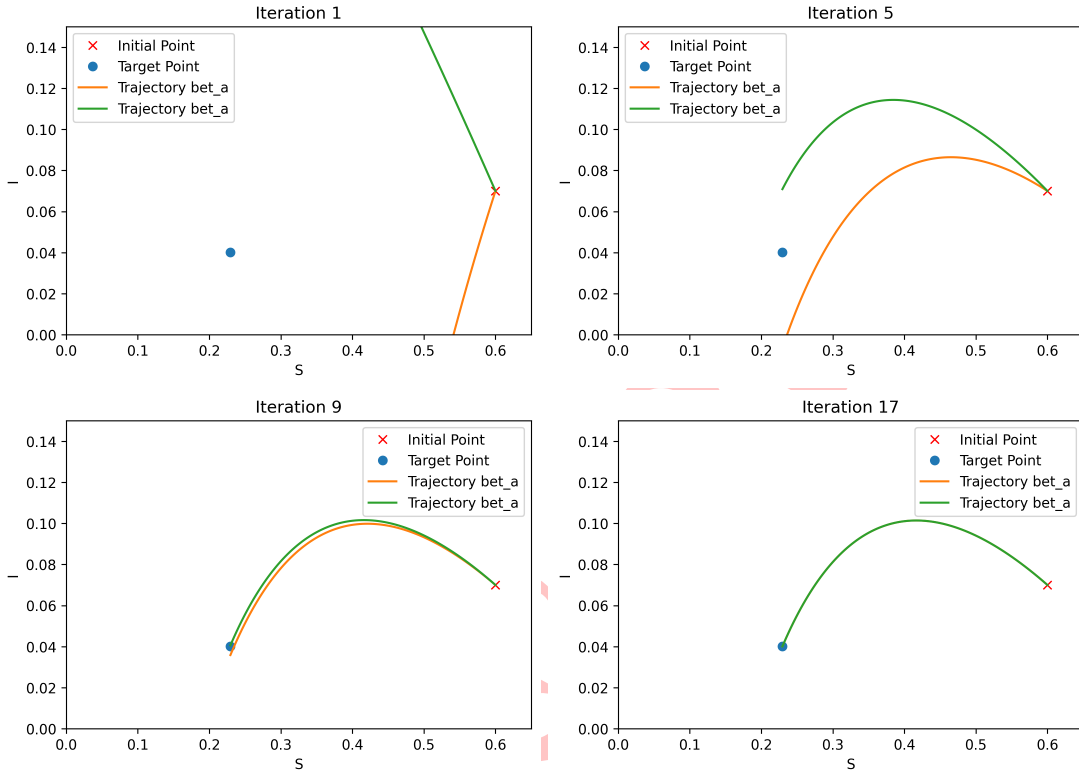


**Figure 1:** Dichotomy-like approach with a precision of  $\varepsilon = 10^{-6}$

of defining this region (see Algorithm 4) and subsequently employing the Newton-Raphson method to solve equation (42) for  $\tau$ , from which  $T = \log(\tau)$  is computed. With  $T$  determined, attaining  $I(T) = I_d$  is guaranteed. Given that multiple parameter combinations satisfy this condition, we formulate the optimization problem:

$$\min_{(a,b_1,b_2) \in \text{Region}} |S(T) - S_d|,$$

which is addressed numerically using a technique analogous to that outlined in Algorithm 2. To avoid redundancy, we refrain from restating the algorithm here but note that it now involves optimizing three parameters. Consequently, rather than restricting the search to a single interval, we investigate parameter values within two spherical regions centered at randomly selected points  $P_0$  and  $Q_0$  within the feasible region.

It is noteworthy that convergence to an optimal solution is not assured, owing to the problem's intrinsic properties and the non-uniform structure of the feasible region (see Fig. 5). A particular challenge is the potential for stagnation if the initial points  $P_0$  and  $Q_0$  are positioned in areas of minimal variation in the objective function or are insufficiently separated, risking convergence to a suboptimal local minimum. Nevertheless, a significant advantage of this method lies in its independence from directly solving differential system (3), thereby reducing computational demands. Another advantage of this approach is the possibility of estimating the exact time for reaching a specific number of infective individuals if  $a, b_1$  and  $b_2$  are chosen correctly. As evidenced in Table 2, the algorithm successfully identifies a solution

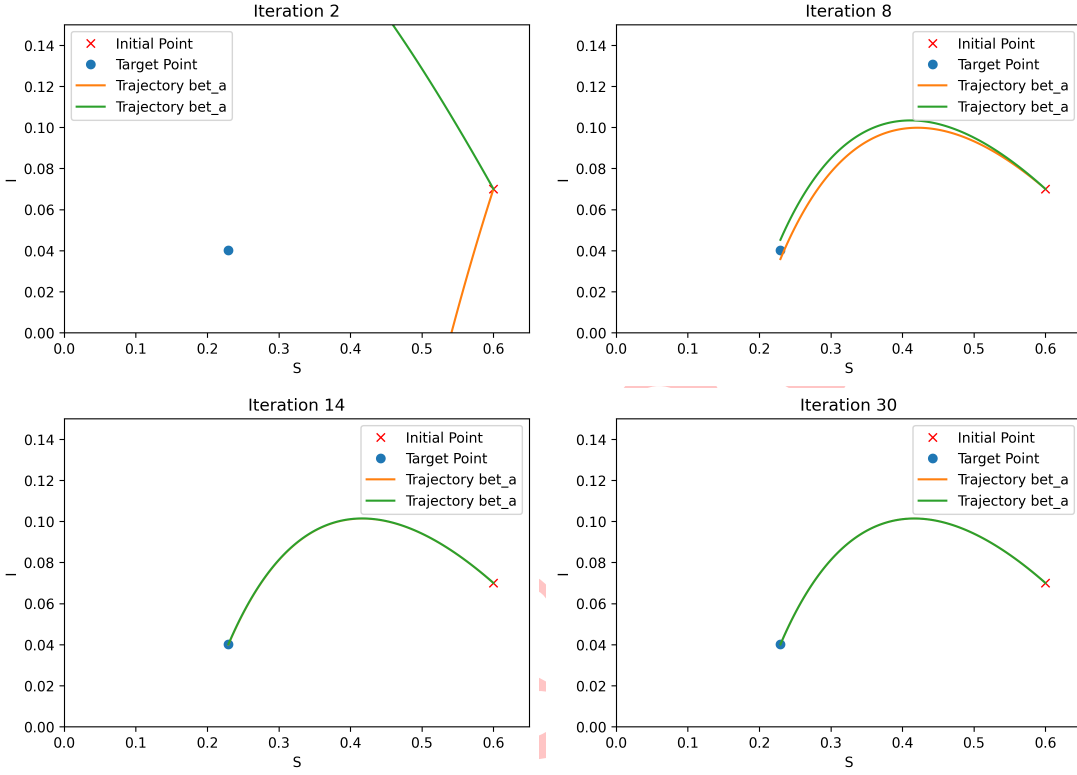


**Figure 2:** Dichotomy-like approach with a precision of  $\varepsilon = 10^{-10}$

---

**Algorithm 4 :** Admissible Region:  $a, b_1$  and  $b_2$

---

- 1: **Require:**  $\beta_0, m, \rho, S_d, I_d, S_0, I_0, T_{\max}, dt, \lambda$
  - 2: **Generate array of values for:**  $a, b_1$ , and  $b_2$
  - 3:  $A \leftarrow [0 : \max A], B_1 \leftarrow [1 : \max B_1], B_2 \leftarrow [1 : \max B_2]$
  - 4: **for**  $a_i \in A$  **do**
  - 5:   **for**  $b1_j \in B_1$  **do**
  - 6:     **for**  $b2_k \in B_2$  **do**
  - 7:       Region  $\leftarrow (a_i, b1_j, b2_k)$
  - 8:     **end for**
  - 9:   **end for**
  - 10: **end for**
  - 11: **Output:** best match among regions
- 

that facilitates partial disease control by achieving  $I_d$ , and in select cases, accomplishes full control by approximating  $S_d$  through an integrated analytical and algorithmic approach.

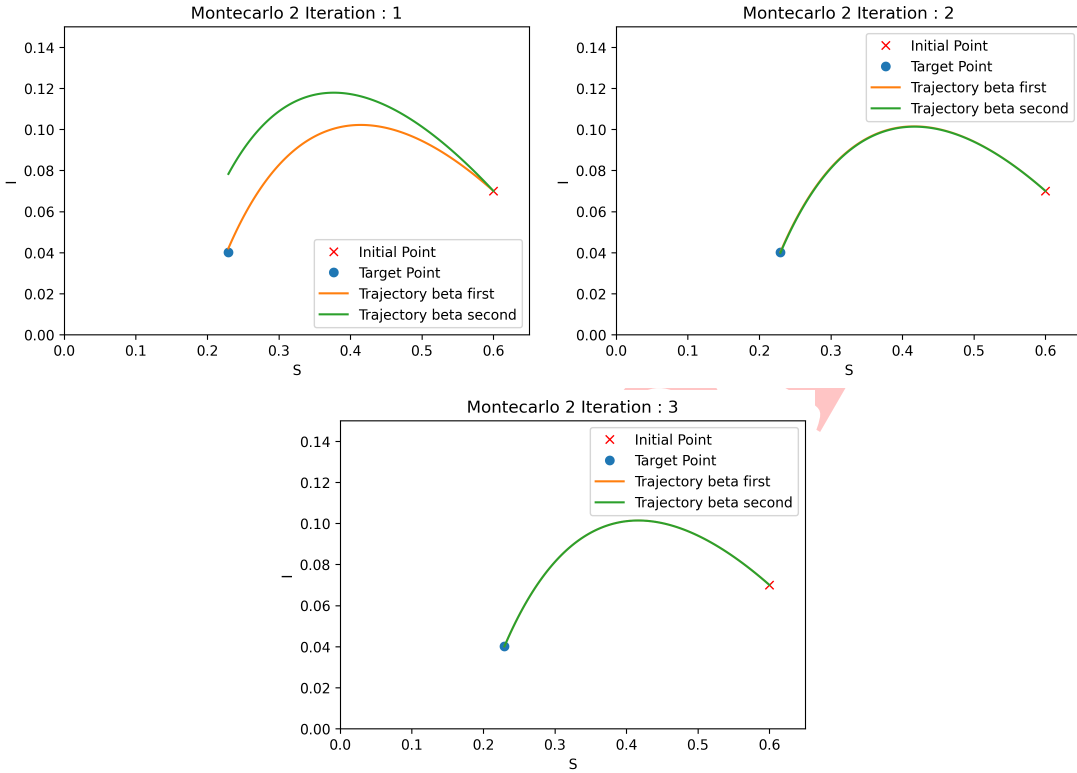


Figure 3: Monte Carlo 2 : precision  $\varepsilon = 10^{-6}$

## Conclusion and Perspectives

In this study, we have developed a comprehensive framework for controlling epidemic dynamics using the SIR model. By introducing a time-varying incidence rate, we established the global controllability of the nonlinear system, providing a theoretical foundation for managing disease spread through adaptive interventions. Our explicit solutions for partial control demonstrate the feasibility of precisely managing the infected population at any given time, offering practical guidance for public health strategies. Furthermore, we introduced numerical methods that leverage algorithmic approaches to achieve full control, steering the system toward a desired state  $(S_d, I_d)$  with optimized efficiency. A key innovation of this work is the hybrid method, which integrates analytical solutions from partial control with algorithmic optimization, enhancing both the precision and computational efficiency of epidemic management strategies.

This research bridges the gap between theoretical controllability and practical intervention, providing a robust toolkit for public health decision-making. By advancing both the understanding and implementation of control strategies for nonlinear systems, our findings have the potential to inform more effective and responsive policies for mitigating the impact of infectious diseases.

Looking ahead, our work opens several avenues for future exploration. The hybrid method, which combines analytical insights with algorithmic optimization, could be extended to more complex epidemiological models, such as those incorporating multiple strains, spatial dynamics, or demographic factors.

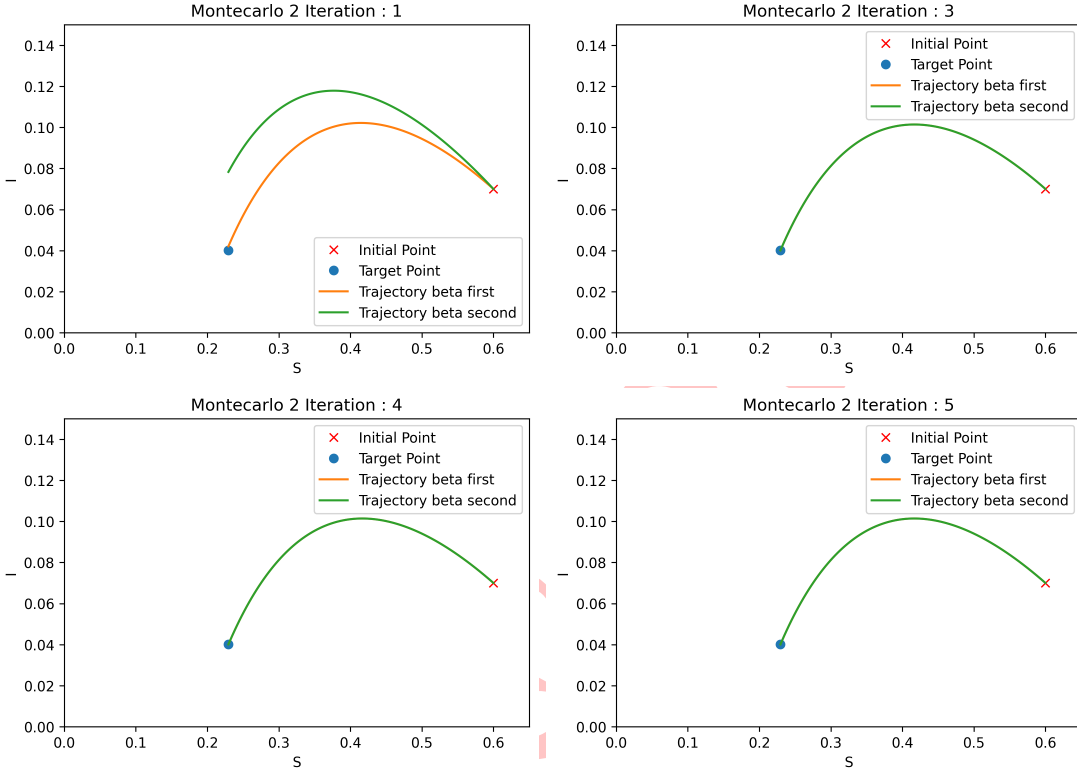


**Figure 4:** Monte Carlo 2 : precision  $\varepsilon = 10^{-10}$

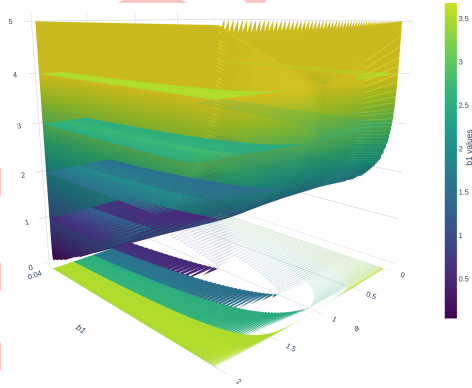


**Figure 5:** The parameters  $a$ ,  $b_1$ , and  $b_2$  were varied within the interval  $[0,5]$ . A 3D search grid with dimensions  $100 \times 100 \times 100$  was employed.

Additionally, integrating real-time data into our control strategies could enhance their adaptability and effectiveness in dynamic, real-world environments. We also see potential in applying our controllability framework to other domains, such as ecological management or economic systems, where similar nonlinear dynamics govern system behavior. Ultimately, this research contributes to the broader goal of developing adaptive and optimized control strategies for complex systems, with far-reaching implications



**Table 2:** Model parameters:  $\beta_0 = 0.3$ ,  $\lambda = 0.1$ ; initial conditions:  $S_0 = 0.8$ ,  $I_0 = 0.2$ ; target values:  $S_d = 0.4$ ,  $I_d = 0.05$ . The Newton-Raphson method was implemented with a convergence tolerance of  $10^{-7}$ .

Initialization	Precision	Iterations	a	$b_1$	$b_2$	$(S_T, I_T)$
P0 (4.27, 0.34, 1.66) Q0 (3.46, 1.30, 3.83)	$10^{-2}$	16	3.05575	0.09121	1.05272	(0.40, 0.05)
P0 (1.47, 0.90, 3.02) Q0 (2.12, 0.29, 0.64)	$10^{-2}$	11	3.09626	0.09121	2.4696	(0.35, 0.05)
P0 (3.98, 1.55, 5.00) Q0 (1.59, 1.45, 4.94)	$10^{-4}$	9	4.3519	0.1418	4.5951	(0.40002, 0.05)
P0 (2.00, 0.19, 0.39) Q0 (2.65, 0.85, 3.07)	$10^{-4}$	9	2.9747	0.0912	4.3421	(0.3653, 0.05)
P0 (4.17, 0.85, 1.35) Q0 (4.23, 0.14, 3.63)	$10^{-6}$	19	4.4329	0.1418	2.6215	(0.40068, 0.05)
P0 (3.66, 0.79, 1.30) Q0 (2.20, 0.90, 3.33)	$10^{-6}$	10	3.7848	0.1418	2.4696	(0.49342, 0.05)

beyond epidemic control.

A promising direction for future research would be to compare the present results with those obtained using machine learning-based methods, particularly neural network architectures developed for epidemic control problems (e.g., [12, 13, 18]). Of particular interest would be the application of supervised learning to approximate or evaluate controllability conditions in cases where the classical Lie bracket approach is inconclusive or computationally intractable. Such data-driven methods could complement analytic techniques and potentially extend the range of systems for which controllability can be rigorously assessed.

## Acknowledgements

This research was supported through computational resources of HPC-MARWAN (www.marwan.ma/hpc) provided by the National Center for Scientific and Technical Research (CNRST), Rabat, Morocco. This work was realised with the support of the CNRST as part of the "PhD-Associate Scholarship - PASS" program.

## References

- [1] V. Andreasen, *The final size of an epidemic and its relation to the basic reproduction number*, Bull. Math. Biol. **73** (2011) 2305–2321.
- [2] N. Bacaër, *A Short History of Mathematical Population Dynamics*, Springer-Verlag London Limited, 2011.

- [3] R. Balderrama, J. Peressutti, J. Pinasco, F. Vazquez, C. Vega, *Optimal control for a SIR epidemic model with limited quarantine*, Sci. Rep. **12**, (2022) 12583.
- [4] L. Boujallal, M. Elhia, O. Balatif, *A novel control set-valued approach with application to epidemic models*, J. Appl. Math. Comp. **65** (2021) 295–319.
- [5] F. Brauer, *The Kermack–McKendrick epidemic model revisited*, Math. Biosci. **198** (2005) 119–131.
- [6] V. Capasso, *Mathematical Structures of Epidemic Systems*. Springer Berlin Heidelberg, 1993.
- [7] A. Carvalho, S. Gonçalves, *An analytical solution for the Kermack–McKendrick model*, Phys. A **566** (2021) 125659.
- [8] D. Clancy, A. Piunovskiy, *An explicit optimal isolation policy for a deterministic epidemic model*, Appl. Math. Comput. **163** (2005) 1109–1121.
- [9] I. Dehaj, A. Dehaj, M. Aziz-Alaoui, M. Rachik, *A new concept of controllability for a class of nonlinear continuous SIR systems*, Chaos Solitons Fract. **192** (2025) 116013.
- [10] O. Diekmann, J. Heesterbeek, J. Metz, *On the definition and the computation of the basic reproduction ratio  $R_0$  in models for infectious diseases in heterogeneous populations*, J. Math. Biol. **28** (1990) 365–382.
- [11] P. van den Driessche, J. Watmough, *Reproduction numbers and sub-threshold endemic equilibria for compartmental models of disease transmission*, Math. Biosci. **180** (2002) 29–48 .
- [12] S. Effati, A. Mansoori, M. Eshaghnezhad, *Linear quadratic optimal control problem with fuzzy variables via neural network*, J. Exp. Theor. AI. **33(2)** (2021) 283–296.
- [13] A. Haluszczynski, C. Räth, *Controlling nonlinear dynamical systems into arbitrary states using machine learning*, Sci. Rep. **11** (2021) 12991.
- [14] N. Hansen, *The CMA evolution strategy: a comparing review*, Towards a New Evolutionary Computation: Studies in Fuzziness and Soft Computing, vol 192, Springer, Berlin, Heidelberg (2006) 75–102.
- [15] N. Hansen, *The CMA evolution strategy: A tutorial*, arXiv preprint arXiv:1604.00772 (2016).
- [16] P. Hartman, *Ordinary Differential Equations*, SIAM (2002).
- [17] J. Heffernan, R. Smith, L. Wahl, *Perspectives on the basic reproductive ratio*, J. R. Soc. Interface **2** (2005) 281–293.
- [18] R. Heydari Dastjerdi, G. Ahmadi, M. Dadkhah, A. Yari, *Optimal control of infectious diseases using artificial neural networks*, Control. Optim. Appl. Math. **8(2)** (2023) 17–32.
- [19] R. Hirschorn, *Controllability in nonlinear systems*, J. Differ. Equ. **19** (1975) 46–61.
- [20] W. Kermack, A. McKendrick, *A contribution to the mathematical theory of epidemics*, Proc. Roy. Soc. Lond. Ser. A. **115** (1927) 700–721.

- [21] C. Michaud, *Global burden of infectious diseases*, Encyclopedia Microbio. **444** (2009).
- [22] R. Morton, K. Wickwire, *On the optimal control of a deterministic epidemic*, Adv. in Appl. Probab. **6** (1974) 622–635.
- [23] Y. Ozaki, S. Takenaga, M. Onishi, *Global search versus local search in hyperparameter optimization*, Proc. IEEE Congr. Evol. Comput. (CEC) (2022) 1–9.
- [24] H. Sussmann, *Nonlinear Controllability and Optimal Control*, Routledge (2017).
- [25] M. Turkyilmazoglu, *Explicit formulae for the peak time of an epidemic from the SIR model*, Phys. D. **422** (2021) 132902.
- [26] K. Wickwire, *Optimal control policies for reducing the maximum size of a closed epidemic—I. Deterministic dynamics*, Math. Biosci. **30** (1976) 129–137.
- [27] O. Zakary, S. Bidah, M. Rachik, *Optimizing infection trajectories: innovation in controllability of nonlinear SIR model*, Rev. Mex. Ing. Bioméd. **45** (2024) 151–171.